

Knotted Solutions of Maxwell's Equations

Pushkal Shrivastava
MS10084

A dissertation for partial fulfilment of BS-MS



Indian Institute of Science Education and Research Mohali
April 2015

Certificate of Examination

This is to certify that the dissertation titled "**Knotted Solutions of Maxwell's Equations**" submitted by Mr. **Pushkal Shrivastava** (Reg No.MS10084) for the partial fulfilment of MS degree programme of the Institute, has been examined by the thesis committee duly appointed by the Institute. The committee finds the work done by the candidate satisfactory and recommends the report to be accepted.

Prof. Charanjit Singh Aulakh
(Supervisor)

Prof. Jasjeet Singh Bagla

Dr. Harvinder Kaur Jassal

Dated: 24-04-2015

Declaration

This work presented in the dissertation has been carried out by me under the guidance of Prof. Charanjit Singh Aulakh at the Indian Institute of Science Education, Mohali.

This work has not been submitted in part or in full for a degree, or diploma or a fellowship to other university or institute. Whenever contributions of others are involved, every effort is made to indicate this clearly, with due acknowledgement of collaborative research and discussions. This thesis is a bona fide record of original work done by me and all sources listed within have been detailed in the bibliography.

Pushkal Shrivastava
(Candidate)

Dated: 24-04-2015

In my capacity as the the supervisor of the candidate's project work, I certify the above statements by the candidate are true to the best of my knowledge.

Prof. Charanjit Singh Aulakh
(Supervisor)

Acknowledgement

I am glad to have undertaken this thesis and explored many interesting topics. The successful completion of the thesis wouldn't have been possible without the support from various sources. I am grateful to my supervisor, Prof. Charanjit Singh Aulakh for giving me the opportunity to work on this interesting problem and guiding me throughout the thesis. I would also like to thank the IISER Mohali and especially the Physics Department for their support.

Pushkal Shrivastava
(Candidate)

List of Figures

2.1	A torus. 'A' is a meridian curve, 'B' is a longitude curve.	7
2.2	A (2,3) torus knot. Also known as Trefoil Knot.	8
2.3	Visualising K	9
2.4	Stereographic Projection: $S^2 \rightarrow R^2$	9
2.5	Parametric plot for $p = 2$ and $q = 3$ gives a (2,3) torus knot.	10
3.1	core field lines for $p=1, q=1$	12
3.2	core field lines for $p=2, q=3$	12
3.3	$\psi_B = 0.45$ and $\psi_B = -0.45$ for $p=1, q=1$	12
3.4	$\psi_B = 0.45$ and $\psi_B = 0$ for $p=1, q=1$	13
3.5	$\psi_B = 0$ for $p=2, q=3$	13
3.6	$\psi_B = 0.1$ and $\psi_B = -0.1$ for $p=2, q=3$	13
3.7	time evolution of surfaces $\psi_B = 0.45$ and $\psi_B = -0.45$ for $p=1, q=1$. Time $t=-1, t=0$ and $t=1$ respectively	14
3.8	time evolution of surface $\psi_B = 0.1$ for $p=2, q=3$. Time $t=-1, t=0$ and $t=1$ respectively	14
3.9	time evolution of energy iso-surface for $p=1, q=1$. Time $t=-3, t=0$ and $t=3$ respectively	14
3.10	time evolution of energy iso-surface for $p=2, q=3$. Time $t=-3, t=0$ and $t=3$ respectively	15
3.11	Graph for energy density vs r for $p=1, q=1$ at time $t=0$	15
3.12	Graph for energy density vs ρ for $p=2, q=3$ at time $t=0$	15
3.13	Dependence of energy density on x for $a = 1$	16
3.14	Dependence of energy density on x for $a = 2$	16
3.15	Dependence of energy density on y for $a = 1$	17
3.16	Dependence of energy density on z for $a = 2$	17
4.1	Reflection of plane wave	20
4.2	Computing retarded potentials	21
4.3	$\psi_B^r = 0.45$ and $\psi_B^r = -0.45$ for $p = 1$ and $q = 1$	23
4.4	Evolution of energy iso-surfaces of total electromagnetic field. $t = -2, t = 0$ and $t = 2$ respectively.	24
4.5	Evolution of surface charge density. $t = 0$ and $t = 1$ respectively.	24
4.6	Evolution of surface current density. $t = 0$ and $t = 1$ respectively.	24

4.7	Trajectory of a particle in presence of knotted field.	25
4.8	Velocity vs time. Red is x component of velocity, green is y and blue is z	25
4.9	Induced emf due to the presence of knotted field.	26

Contents

List of Figures	i
Abstract	v
1 Introduction	1
1.1 Bateman's construction	1
1.2 Putting the constants back	5
2 Knots	7
2.1 Torus knots	7
2.2 Singular Points on a Complex Hyper-surfaces	8
3 Knotted Solutions	11
4 Properties	19
4.1 Reflection	19
4.2 Particle Trajectory	25
4.3 Emf induced	26
5 Formalism	27
5.1 Covariant Formalism	27
5.2 Map to $SU(2)$ gauge theories	28
5.3 Gauge Transformation	29
Bibliography	30

Abstract

Presented here are recently proposed null solutions of source free Maxwell's Equations wherein field lines encode all p,q torus knots and links. Some classical properties such as reflection, trajectory of a charged particle in the field and emf induced in a loop of wire due to the presence of field have been studied. Attempts towards generalization to non-abelian gauge theories have been made.

Chapter 1

Introduction

The whole of electrodynamics is governed by Maxwell's equations, together with Lorentz force law. Maxwell's equations:

$$\nabla \cdot \mathbf{E} = \frac{\rho}{\epsilon_0} \quad (1.1a)$$

$$\nabla \cdot \mathbf{B} = 0 \quad (1.1b)$$

$$\nabla \times \mathbf{E} = -\frac{\partial \mathbf{B}}{\partial t} \quad (1.1c)$$

$$\nabla \times \mathbf{B} = \left(\mu_0 \mathbf{J} + \frac{1}{c^2} \frac{\partial \mathbf{E}}{\partial t} \right) \quad (1.1d)$$

Lorentz Force Law:

$$\mathbf{F} = q(\mathbf{E} + \mathbf{v} \times \mathbf{B}) \quad (1.2a)$$

A solution is termed null when following conditions are satisfied.

$$\mathbf{E} \cdot \mathbf{E} - \mathbf{B} \cdot \mathbf{B} = 0 \quad (1.3a)$$

$$\mathbf{E} \cdot \mathbf{B} = 0 \quad (1.3b)$$

1.1 Bateman's construction

To construct the knotted solutions, we would first require a formalism called Bateman's construction[1][2]. Let us define a complex vector field with the real part as electric field and the imaginary part as magnetic field.

$$\mathbf{F} = \mathbf{E} + i\mathbf{B} \quad (1.4)$$

The source-less Maxwell's equations (suppressing the constants) can be re-written in terms of \mathbf{F} as:

$$\nabla \cdot \mathbf{F} = 0 \quad (1.5a)$$

$$\nabla \times \mathbf{F} = i \frac{\partial \mathbf{F}}{\partial t} \quad (1.5b)$$

The real part of equation 1.5(a) is same as equation 1.1 (a) and imaginary part gives equation 1.1 (b). The right hand side of equation 1.5 (b) simplifies to $-\frac{\partial \mathbf{B}}{\partial t} + i \frac{\partial \mathbf{E}}{\partial t}$. Hence the real part of the equation would give equation 1.1 (c) and the imaginary part would result in equation 1.1 (4).

The null condition can be expressed as follows.

$$\mathbf{F} \cdot \mathbf{F} = 0 \quad (1.6)$$

The real part of this equation gives equation 1.3 (a) and the imaginary part gives 1.3 (b).

Defining 2 complex scalars α and β with the following constraint.

$$\nabla \alpha \times \nabla \beta = i (\partial_t \alpha \nabla \beta - \partial_t \beta \nabla \alpha) \quad (1.7)$$

This is the called the Bateman's condition. If we define,

$$\mathbf{F} = \nabla \alpha \times \nabla \beta \quad (1.8)$$

We can show that \mathbf{F} defined above satisfies equations 1.5 through 1.6. Hence \mathbf{F} defines a null solution of source-less Maxwell's equations.

Null Condition:

$$\begin{aligned} \mathbf{F} \cdot \mathbf{F} &= \nabla \alpha \times \nabla \beta \cdot \nabla \alpha \times \nabla \beta \\ &= \nabla \alpha \times \nabla \beta \cdot i (\partial_t \alpha \nabla \beta - \partial_t \beta \nabla \alpha) \\ &= 0 \end{aligned}$$

We have used equation 1.7 in the second step.

Divergence Condition:

$$\begin{aligned} \nabla \cdot \mathbf{F} &= \nabla \cdot (\nabla \alpha \times \nabla \beta) \\ &= \nabla \beta \cdot (\nabla \times \nabla \alpha) - \nabla \alpha \cdot (\nabla \times \nabla \beta) \\ &= 0 \end{aligned}$$

Curl Condition.

$$\begin{aligned}
\nabla \times \mathbf{F} &= \nabla \times (\nabla\alpha \times \nabla\beta) \\
&= \nabla \times i(\partial_t\alpha\nabla\beta - \partial_t\beta\nabla\alpha) \\
&= i(\partial_t\alpha(\nabla \times \nabla\beta) + \partial_t(\nabla\alpha) \times \nabla\beta - \partial_t\beta(\nabla \times \nabla\alpha) - \partial_t(\nabla\beta) \times \nabla\alpha) \\
&= i(\partial_t(\nabla\alpha) \times \nabla\beta + \nabla\alpha \times \partial_t(\nabla\beta)) \\
&= i\partial_t(\nabla\alpha \times \nabla\beta) \\
&= i\partial_t\mathbf{F}
\end{aligned}$$

We have used the following properties of curl and divergence.

$$\begin{aligned}
\nabla \cdot (\mathbf{A} \times \mathbf{B}) &= \mathbf{B} \cdot (\nabla \times \mathbf{A}) - \mathbf{A} \cdot (\nabla \times \mathbf{B}) \\
\nabla \times (f\mathbf{A}) &= f(\nabla \times \mathbf{A}) - \mathbf{A} \times (\nabla f) \\
\nabla \times \nabla f &= 0
\end{aligned}$$

Clearly, \mathbf{F} defined in equation 1.8 along with the Bateman's condition, equation 1.7, defines a null solution to the source free Maxwell's equations. This approach was developed by Bateman and hence it is called Bateman's construction.

Now consider any 2 holomorphic functions f and g of α and β . It can be shown that f and g would also satisfy Bateman's conditions. Therefore, these new complex scalars would also give rise to a null solution of Maxwell's equations.

$$\begin{aligned}
\nabla f &= \partial_\alpha f \nabla\alpha + \partial_\beta f \nabla\beta \\
\partial_t f &= \partial_\alpha f \partial_t\alpha + \partial_\beta f \partial_t\beta
\end{aligned}$$

We have similar equations for g . Using these equations we can write.

$$\begin{aligned}
\nabla f \times \nabla g &= (\partial_\alpha f \nabla\alpha + \partial_\beta f \nabla\beta) \times (\partial_\alpha g \nabla\alpha + \partial_\beta g \nabla\beta) \\
&= (\partial_\alpha f \partial_\beta g - \partial_\beta f \partial_\alpha g) \nabla\alpha \times \nabla\beta \\
&= i(\partial_\alpha f \partial_\beta g - \partial_\beta f \partial_\alpha g) (\partial_t\alpha \nabla\beta - \partial_t\beta \nabla\alpha)
\end{aligned}$$

$$\begin{aligned}
i(\partial_t f \nabla g - \partial_t g \nabla f) &= i((\partial_\alpha f \partial_t\alpha + \partial_\beta f \partial_t\beta) (\partial_\alpha g \nabla\alpha + \partial_\beta g \nabla\beta) - (\partial_\alpha g \partial_t\alpha + \partial_\beta g \partial_t\beta) (\partial_\alpha f \nabla\alpha + \partial_\beta f \nabla\beta)) \\
&= i(\partial_\alpha f \partial_\beta g - \partial_\beta f \partial_\alpha g) (\partial_t\alpha \nabla\beta - \partial_t\beta \nabla\alpha)
\end{aligned}$$

Hence we get the desired result.

$$\nabla f \times \nabla g = i(\partial_t f \nabla g - \partial_t g \nabla f)$$

The new solution F' is related to the old solution F by.

$$\mathbf{F}' = (\partial_\alpha f \partial_\beta g - \partial_\beta f \partial_\alpha g) \mathbf{F}$$

So every α and β gives a family of solutions. Moreover, all related solutions have same normalized Poynting vector.

Plane-wave solutions

Consider $\alpha = z - t$, $\beta = x + iy$, $f = e^{i\alpha}$ and $g = \beta$. We have,

$$\partial_t \alpha = -1$$

$$\partial_t \beta = 0$$

$$\nabla \alpha = (0, 0, 1)$$

$$\nabla \beta = (1, i, 0)$$

Checking Bateman's condition.

$$\nabla \alpha \times \nabla \beta = (-i, 1, 0)$$

$$i(\partial_t \alpha \nabla \beta - \partial_t \beta \nabla \alpha) = (-i, 1, 0)$$

As α and β satisfy Bateman's conditions, so does f and g . F defined by f and g becomes,

$$\mathbf{F} = (e^{i(z-t)}, ie^{i(z-t)}, 0)$$

$$\mathbf{E} = (\cos(z-t), -\sin(z-t), 0)$$

$$\mathbf{B} = (\sin(z-t), \cos(z-t), 0)$$

Clearly, this is a circularly polarized plane wave solution.

1.2 Putting the constants back

Consider the source free Maxwell's equations. If we make the transformation $E' = E/c$ and $B' = B$, then we can re-write the Maxwell's equations as follows.

$$\nabla \cdot \mathbf{E}' = 0 \quad (1.21a)$$

$$\nabla \cdot \mathbf{B}' = 0 \quad (1.21b)$$

$$\nabla \times \mathbf{E}' = -\frac{1}{c} \frac{\partial \mathbf{B}'}{\partial t} \quad (1.21c)$$

$$\nabla \times \mathbf{B}' = \frac{1}{c} \frac{\partial \mathbf{E}'}{\partial t} \quad (1.21d)$$

Just as before, defining $F' = E' + iB'$. Equation 1.5(b) can be expressed as follows.

$$\nabla \times \mathbf{F}' = \frac{i}{c} \frac{\partial \mathbf{F}'}{\partial t} = i \frac{\partial \mathbf{F}'}{\partial(ct)} \quad (1.22)$$

If we have solutions to the equation $\nabla \times \mathbf{F} = i \frac{\partial \mathbf{F}}{\partial t}$, then we can obtain the solutions to equation 1.22 by simply replacing t by ct .

$$\mathbf{F}'(x, y, z, t) = \mathbf{F}(x, y, z, ct)$$

This would give the following as electric and magnetic field in SI units.

$$\mathbf{E} = c \operatorname{Re}[\mathbf{F}(x, y, z, ct)] \quad (1.23a)$$

$$\mathbf{B} = \operatorname{Im}[\mathbf{F}(x, y, z, ct)] \quad (1.23b)$$

The space-time coordinates are dimension-full. Hence there must be an implicit scale factor a associated with the variables x, y, z and ct . That is, $x = x'/a$ where x' has dimensions of [L] and a is some arbitrary length scale.

Chapter 2

Knots

Any closed curve embedded in three dimensional Euclidean space is called a knot. A link of m components consists of m disjoint knots. The formal definition is given below[3].

Definition 1. A **link** L of m components is a subset of S^3 , or of R^3 , that consists of m disjoint, piecewise linear, simple closed curves. A link of one component is called a **knot**.

The simplest example of a knot is a circle.

2.1 Torus knots

Definition 2. A **torus** is a surface of revolution generated by revolving a circle in three dimensional space about an axis coplanar to the circle.

Definition 3. A **meridian curve** is a curve that bounds a disk in the interior of torus but doesn't bound a disk on the surface of torus. A **longitude curve** is a curve that intersect a meridian curve exactly once.

A torus can also be obtained from a rectangle by first forming a cylinder and then joining the open ends of the cylinder, so that it closes on itself.[4]

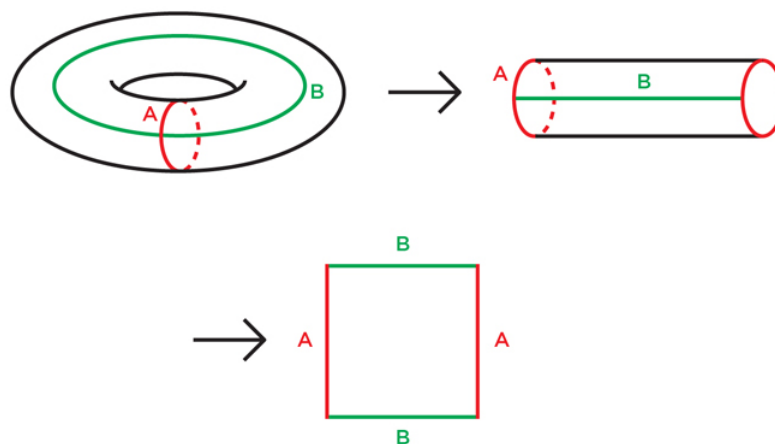


Figure 2.1: A torus. 'A' is a meridian curve, 'B' is a longitude curve.

Definition 4. A (p,q) torus knot is a knot on the surface of torus that goes around p times in the meridian direction and q times in the longitude direction.

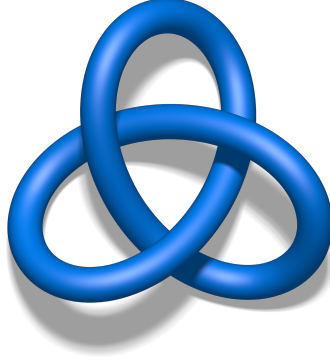


Figure 2.2: A $(2,3)$ torus knot. Also known as Trefoil Knot.

If p and q are co-prime, then we get a knot, else we get a link with m components, with $m = \gcd(p, q)$.

2.2 Singular Points on a Complex Hyper-surfaces

Topology around a singular point on a complex hyper-surface can be non-trivial. This was studied in great detail by J. Milnor[5]. Consider the following function of 2 complex variables.

$$f(z_1, z_2) = z_1^p + z_2^q \quad (2.1)$$

where p and q are positive integers. Defining V to be the hyper-surface spanned by (z_1, z_2) such that $f(z_1, z_2) = 0$. A singular point of a function is a point where all the directional derivatives are zero. For the function f , the singular point lies at origin. 2 complex variables span a 4 dimensional space. The hyper-surface V is a 2 dimensional surface (as $f = 0$ gives 2 constraints. One each for real and imaginary part.) embedded in 4 dimensional space. Consider a point z_0 on V . On taking intersection of a sphere centred at z_0 with V , we get a curve. We would expect this curve to be homeomorphic to circle. But if z_0 is a singular point then the curve can have a more complicated topology. For instance, if we choose the centre to be origin, we would get p,q torus knot as the curve.

$$V = \{(z_1, z_2) \mid z_1^p + z_2^q = 0\} \quad (2.2)$$

$$S_\epsilon = \{(z_1, z_2) \mid |z_1|^2 + |z_2|^2 = \epsilon^2\} \quad (2.3)$$

$$K = V \cap S_\epsilon \quad (2.4)$$

To find the loci of K , let us assume $z_1 = \eta e^{iq\theta}$. Then from the condition $z_1^p + z_2^q = 0$ we find that $z_2^q = -\eta^p e^{ip\theta}$. This gives, $z_2 = \eta^{p/q} e^{(ip\theta + i\pi/q)}$. The condition $|z_1|^2 + |z_2|^2 = \epsilon^2$ becomes

$(\eta^p/q)^2 + \eta^2 = \epsilon^2$. This fixes η in terms of *epsilon*. Hence we get the following.

$$K = \left(\eta e^{iq\theta}, \eta^{p/q} e^{(ip\theta + i\pi/q)} \right) \quad (2.5)$$

K is a curve with parameter θ . To visualise this curve, consider the following figure.

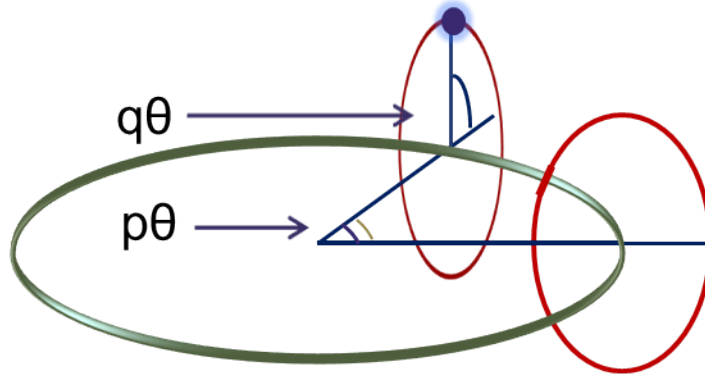


Figure 2.3: Visualising K

$\theta = 0$ correspond to the point on the far right of the red circle parallel to the plane of paper. A non-zero θ corresponds to a point on the circle obtained by revolving the red circle by an angle of $p\theta$ about an axis perpendicular to the plane of green circle and passing through its centre. In the plane of red circle, the point corresponding to θ is obtained via a rotation by an angle of $q\theta$. As θ goes from zero to 2π , the path traced by the point crosses every meridian curve and longitude curve p times and q times respectively and then closes on itself. Hence it is indeed a p, q torus knot.

The curve lies on the 3-sphere S_ϵ . To visualise the curve, we can also take the stereographic projection of S^3 on R^3 . A stereographic projection of 2-sphere on a plane passing through the centre is obtained as follows. Choose any point P on the sphere. Consider the line l joining the north-pole N and P . The point of intersection (R) of l with the plane passing through the centre is the projection of P . Stereographic projection in higher dimensions is just a trivial extension of this concept.

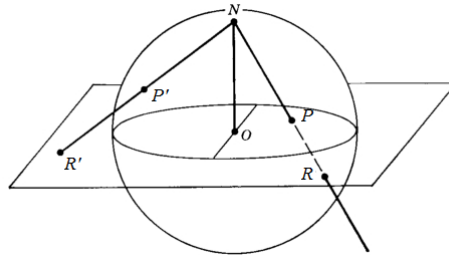


Figure 2.4: Stereographic Projection: $S^2 \rightarrow R^2$

For 3-sphere of unit radius, the form of stereographic projection in terms of complex variables is the

following. Stereographic Projection:

$$z_1 = \frac{r^2 - 1 + 2iz}{r^2 + 1} \quad (2.6a)$$

$$z_2 = \frac{2(x - iy)}{r^2 + 1} \quad (2.6b)$$

where x, y, z are the Cartesian coordinates and r is the distance from origin. Using equation 2.5 with $\epsilon = 1$, we can write x, y, z in terms of parameter θ and constant η .

Stereographic Projection of curve K :

$$x = \frac{1}{2} \sin\left(\frac{\pi}{6} - \theta p\right) \eta^{p/q} \left(\frac{\eta \cos(\theta q) + 1}{1 - \eta \cos(\theta q)} + 1\right) \quad (2.7a)$$

$$y = -\frac{1}{2} \cos\left(\frac{\pi}{6} - \theta p\right) \eta^{p/q} \left(\frac{\eta \cos(\theta q) + 1}{1 - \eta \cos(\theta q)} + 1\right) \quad (2.7b)$$

$$z = \eta \sin(q\theta) \left(\frac{\eta \cos(\theta q) + 1}{1 - \eta \cos(\theta q)} + 1\right) \quad (2.7c)$$

A parameter plot for $p = 2$ and $q = 3$ gives the following. This shows that we can obtain a torus

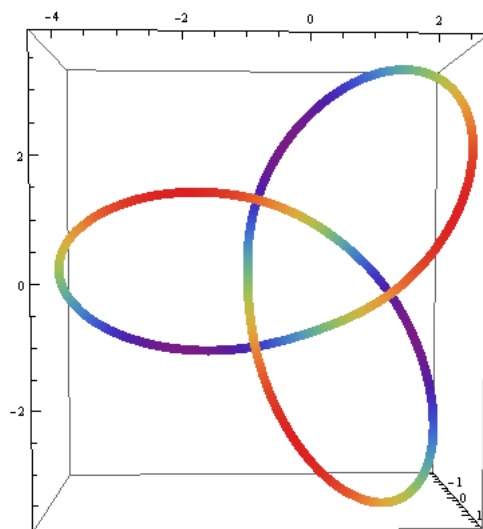


Figure 2.5: Parametric plot for $p = 2$ and $q = 3$ gives a $(2,3)$ torus knot.

knot in three dimensions by taking the intersection of the hyper-surface V with a 3-sphere centred at the singular point; origin.

Chapter 3

Knotted Solutions

Consider the following definition of Bateman's variables.[2][6]

$$\alpha = \frac{r^2 - t^2 + 2iz - 1}{r^2 - (t - i)^2} \quad (3.1a)$$

$$\beta = \frac{2(x - iy)}{r^2 - (t - i)^2} \quad (3.1b)$$

Checking if Bateman's condition, equation 1.7, is satisfied.

$$\nabla\alpha \times \nabla\beta = \begin{pmatrix} \frac{4x(it - iz + 1)}{(-t^2 + 2it + x^2 + y^2 + z^2 + 1)^2} \\ \frac{4y(it - iz + 1)}{(-t^2 + 2it + x^2 + y^2 + z^2 + 1)^2} \\ -\frac{2i(t^2 - 2t(z + i) - x^2 - y^2 + z^2 + 2iz - 1)}{(-t^2 + 2it + x^2 + y^2 + z^2 + 1)^2} \end{pmatrix}$$

$$i(\partial_t\alpha\nabla\beta - \partial_t\beta\nabla\alpha) = \begin{pmatrix} \frac{4x(it - iz + 1)}{(-t^2 + 2it + x^2 + y^2 + z^2 + 1)^2} \\ \frac{4y(it - iz + 1)}{(-t^2 + 2it + x^2 + y^2 + z^2 + 1)^2} \\ -\frac{2i(t^2 - 2t(z + i) - x^2 - y^2 + z^2 + 2iz - 1)}{(-t^2 + 2it + x^2 + y^2 + z^2 + 1)^2} \end{pmatrix}$$

As $\nabla\alpha \times \nabla\beta = i(\partial_t\alpha\nabla\beta - \partial_t\beta\nabla\alpha)$, α and β indeed satisfy Bateman's condition. Hence they generate a null solution of source-less Maxwell's equations. Note that at $t = 0$, the definition of α and β coincides with the stereographic projection of 3-sphere on R^3 (equation 2.6). Moreover, we can check that $|\alpha|^2 + |\beta|^2 = 1$. Now choose $f(\alpha, \beta) = \alpha^p$, $g(\alpha, \beta) = \beta^q$. As f and g are holomorphic functions of α and β , they also generate a solution of Maxwell's equations.

$$\mathbf{F} = \nabla\alpha^p \times \nabla\beta^q \quad (3.2)$$

Defining $\psi_B = \text{Re}(\alpha^p \beta^q)$ and $\psi_E = \text{Im}(\alpha^p \beta^q)$. Then it can be shown that $\nabla \psi_B \cdot \mathbf{B} = 0$ and $\nabla \psi_E \cdot \mathbf{E} = 0$. This implies that the electric and magnetic field lines lie on the surfaces described by $\psi_E = \text{constant}$ and $\psi_B = \text{constant}$ respectively. The surfaces of constant ψ_B have a knotted structure. ψ_B takes values from $-(p^p q^q / (p+q)^{p+q})^{1/2}$ to $(p^p q^q / (p+q)^{p+q})^{1/2}$. For the maximum and minimum values, $\psi_B = \text{constant}$ forms a knot of zero thickness. When ψ_B is varied from its maximum/minimum values to zero, the thickness is increased continually. We get a set of nested torus knots over all space. At $t = 0$, we get the following structure for surfaces of constant ψ_B . The surfaces of constant ψ_E also have a similar structure, rotated in space about z-axis by $\pi/2q$.

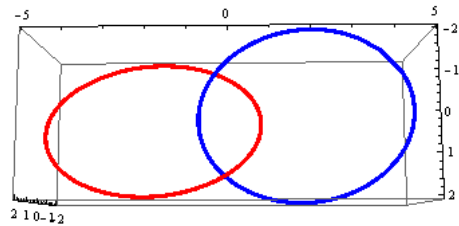


Figure 3.1: core field lines for $p=1, q=1$

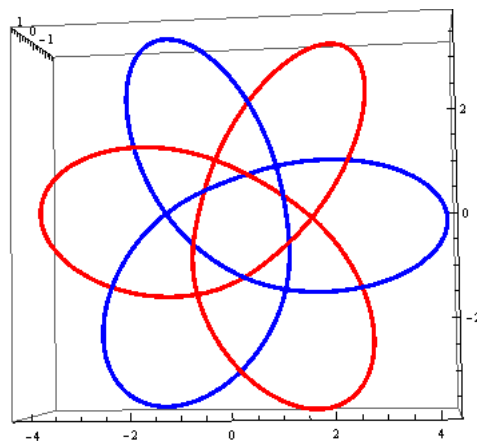


Figure 3.2: core field lines for $p=2, q=3$

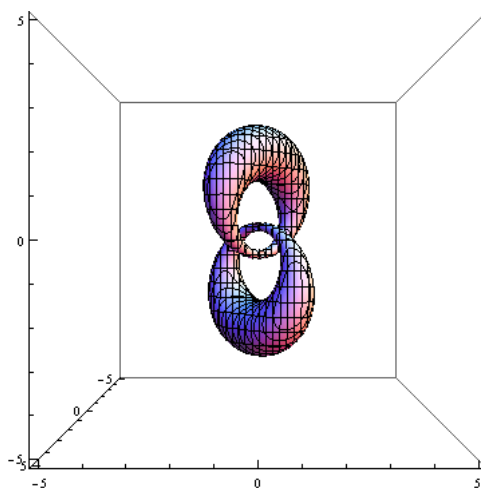


Figure 3.3: $\psi_B = 0.45$ and $\psi_B = -0.45$ for $p=1, q=1$

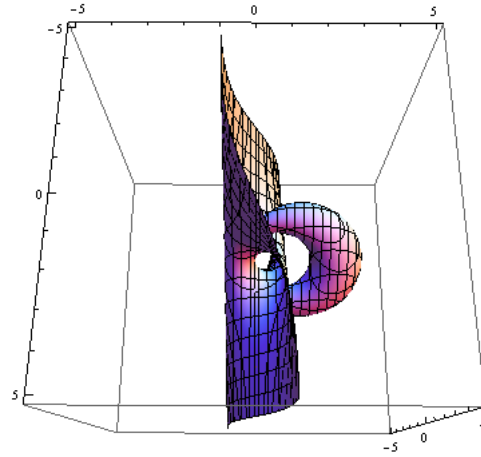


Figure 3.4: $\psi_B = 0.45$ and $\psi_B = 0$ for $p=1, q=1$

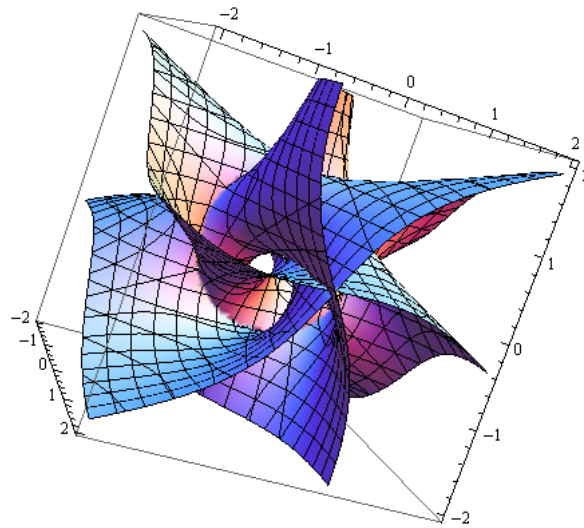


Figure 3.5: $\psi_B = 0$ for $p=2, q=3$

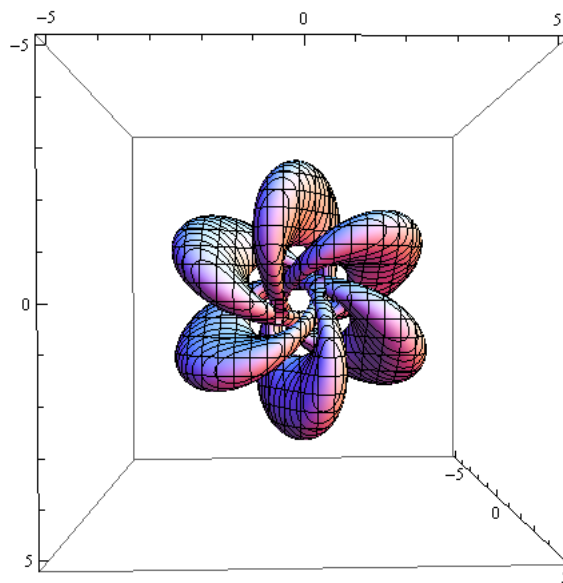


Figure 3.6: $\psi_B = 0.1$ and $\psi_B = -0.1$ for $p=2, q=3$

This knotted structure is preserved in time. As time progresses the surfaces of constant ψ_B twists and turns but retain their basic structure. At all times these surfaces remain homeomorphic to the surfaces at $t = 0$. The energy iso-surfaces propagates in the negative z direction.

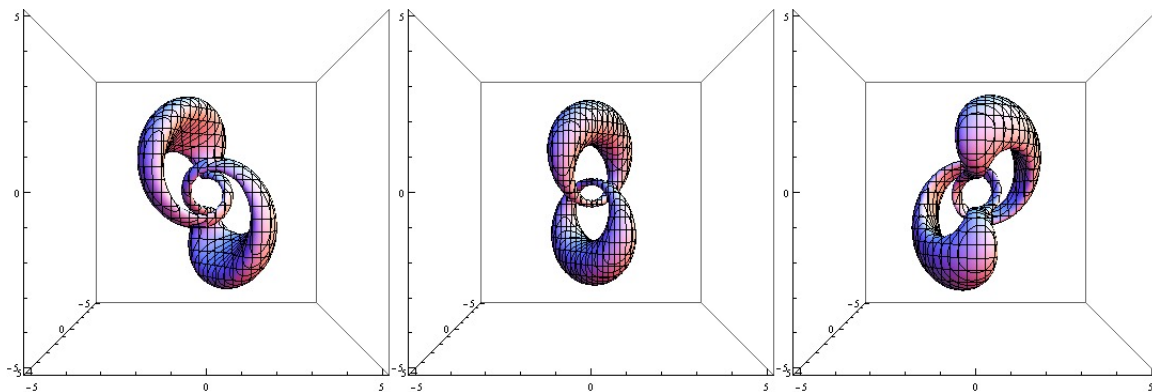


Figure 3.7: time evolution of surfaces $\psi_B = 0.45$ and $\psi_B = -0.45$ for $p=1, q=1$. Time $t=-1, t=0$ and $t=1$ respectively

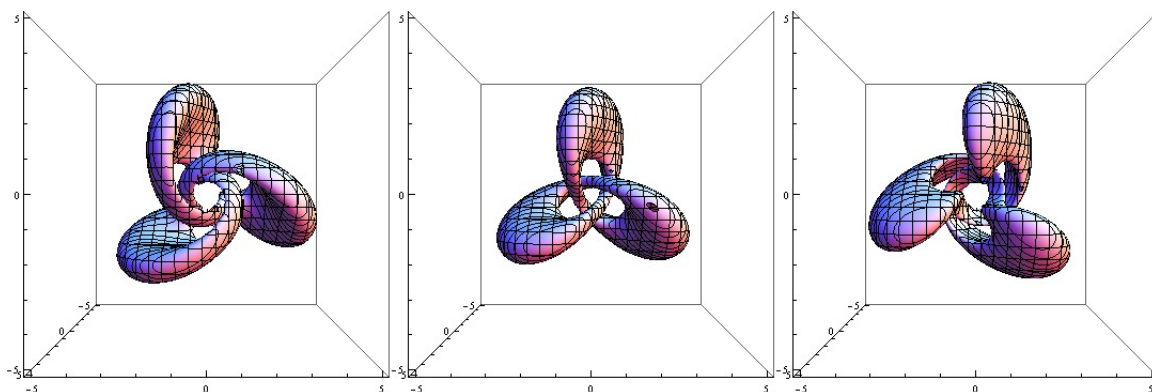


Figure 3.8: time evolution of surface $\psi_B = 0.1$ for $p=2, q=3$. Time $t=-1, t=0$ and $t=1$ respectively

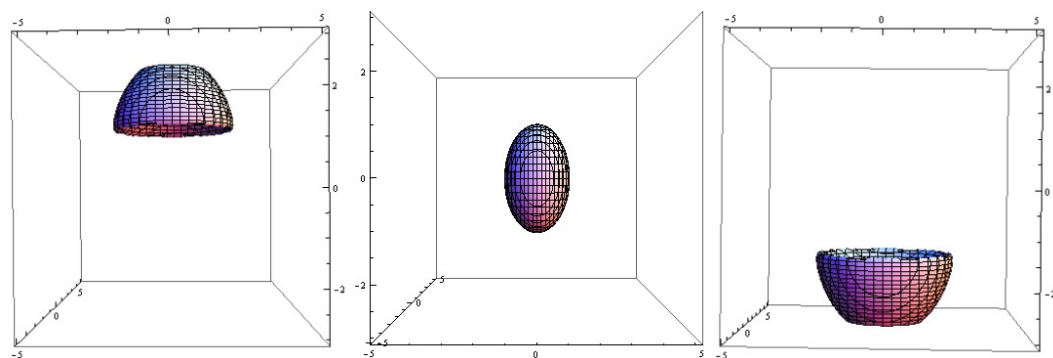


Figure 3.9: time evolution of energy iso-surface for $p=1, q=1$. Time $t=-3, t=0$ and $t=3$ respectively

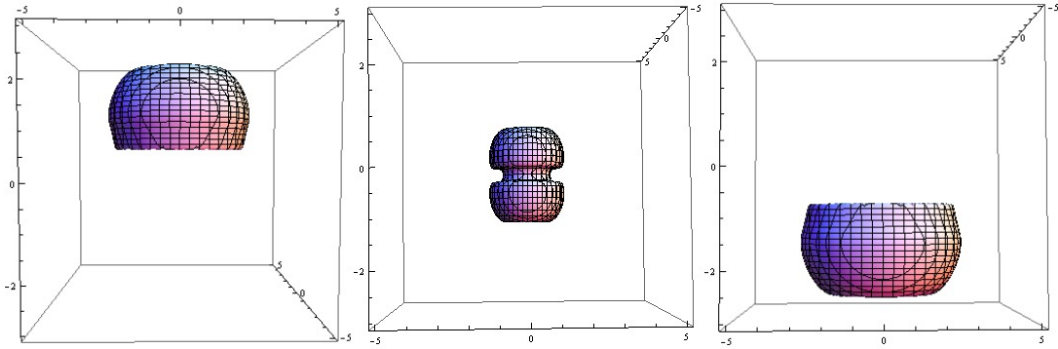


Figure 3.10: time evolution of energy iso-surface for $p=2$, $q=3$. Time $t=-3$, $t=0$ and $t=3$ respectively

Another interesting feature of this solutions is that the energy profile is very dense and falls off rapidly.

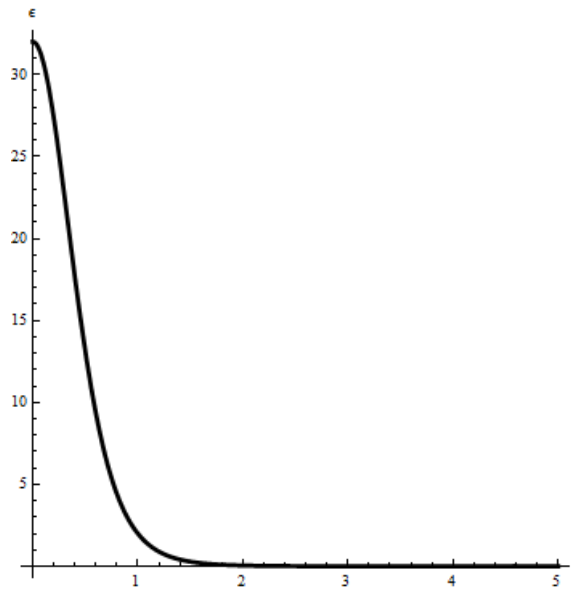


Figure 3.11: Graph for energy density vs r for $p=1$, $q=1$ at time $t=0$

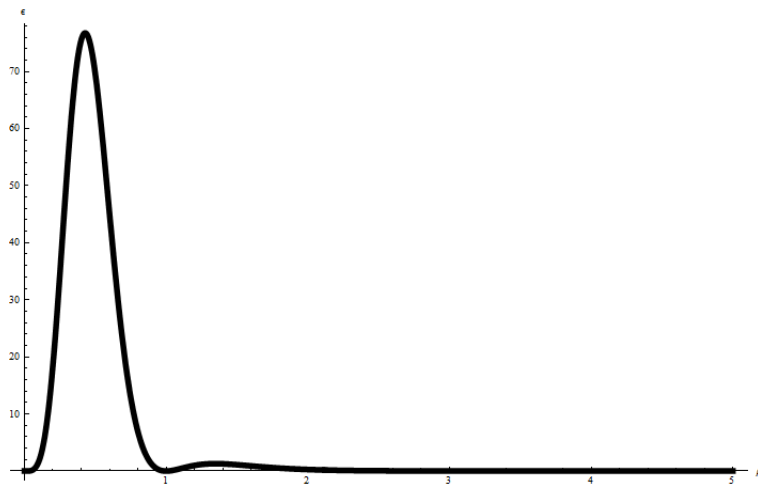


Figure 3.12: Graph for energy density vs ρ for $p=2$, $q=3$ at time $t=0$

The Bateman's construction gives solutions of Maxwell's equations where constants have been suppressed. To get an idea of energy associated with the solutions we need to put back the constants. Using the results in section 1.2, we can get the actual field in terms of the solutions constructed by simply using transformation derived in equation 1.23. This gives the following expression for electric and magnetic field at $t = 0$ for hopfion solution, i.e. $p = 1$ and $q = 1$.

$$\mathbf{E} = ca^2 \left(\frac{4(-x^2 + y^2 + z^2 - a^2)}{(x^2 + y^2 + z^2 + a^2)^3}, \frac{8(az - xy)}{(x^2 + y^2 + z^2 + a^2)^3}, -\frac{8(xz + ay)}{(x^2 + y^2 + z^2 + a^2)^3} \right) \quad (3.3a)$$

$$\mathbf{B} = a^2 \left(\frac{8(xy + az)}{(x^2 + y^2 + z^2 + a^2)^3}, -\frac{4(x^2 - y^2 + z^2 - a^2)}{(x^2 + y^2 + z^2 + a^2)^3}, -\frac{8(ax - yz)}{(x^2 + y^2 + z^2 + a^2)^3} \right) \quad (3.3b)$$

The energy density associated with electromagnetic field is $\frac{1}{2} \left(\epsilon_0 E^2 + \frac{1}{\mu_0} B^2 \right)$. At $t = 0$, it turns out to be,

$$u = \frac{16a^4 \left(a^4 + 2a^2(2x^2 + z^2) + 8axyz + (x^2 + y^2)^2 + 4y^2z^2 + z^4 \right)}{\mu_0 (a^2 + x^2 + y^2 + z^2)^6} \quad (3.4)$$

To get an idea of change in energy profile of the electromagnetic field with time we consider the variation of energy density in a particular direction, with other variables fixed to zero.

$$u(x, 0, 0, t) = \frac{16a^4 \left(a^4 + 2a^2((ct)^2 + 2x^2) + (ct)^4 + x^4 \right)}{\mu_0 \left(a^4 + 2a^2((ct)^2 + x^2) + ((ct)^2 - x^2)^2 \right)^3} \quad (3.5a)$$

$$u(0, y, 0, t) = \frac{16a^4 \left(a^4 + 2a^2(ct)^2 + (ct)^4 + 4(ct)^2y^2 + y^4 \right)}{\mu_0 \left(a^4 + 2a^2((ct)^2 + y^2) + ((ct)^2 - y^2)^2 \right)^3} \quad (3.5b)$$

$$u(0, 0, z, t) = \frac{16a^4}{\mu_0 (a^2 + (ct - z)^2)(a^2 + (ct + z)^2)^3} \quad (3.5c)$$

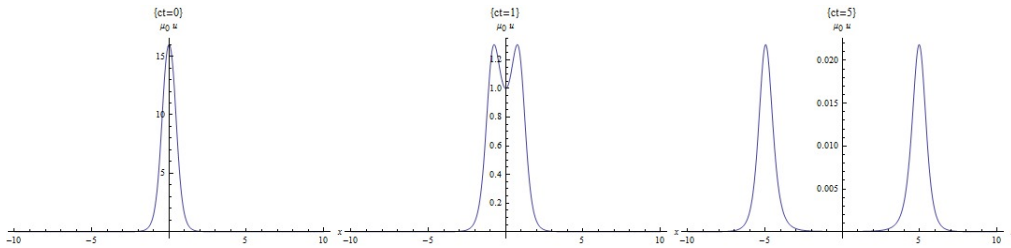


Figure 3.13: Dependence of energy density on x for $a = 1$

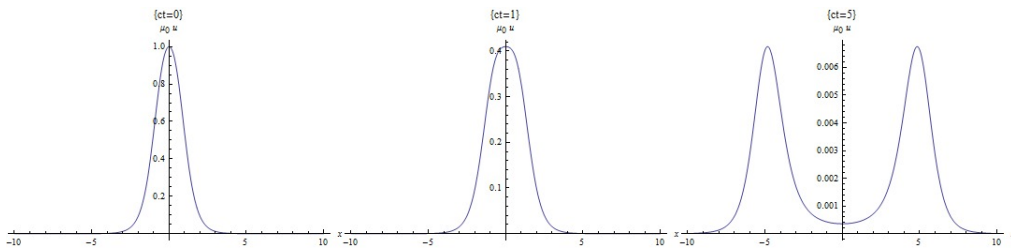


Figure 3.14: Dependence of energy density on x for $a = 2$

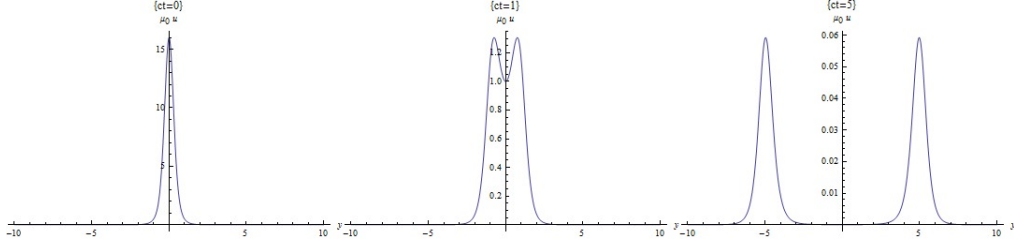


Figure 3.15: Dependence of energy density on y for $a = 1$

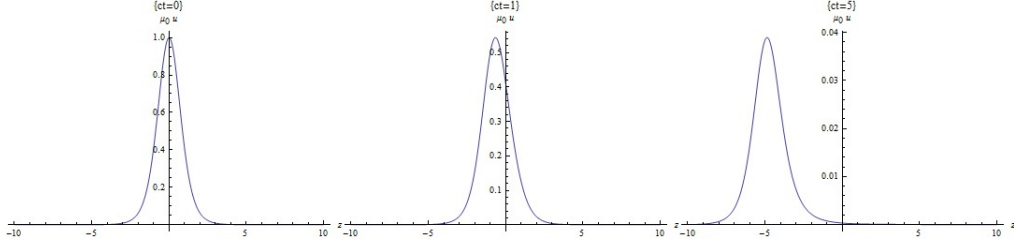


Figure 3.16: Dependence of energy density on z for $a = 2$

From the graphs it is clear that the energy profile is propagating in $-z$ direction at speed of light. As time progresses, the energy profile diffuses in x and y direction and appears to move radially out at speed of light. On increasing the scale a , the energy profile becomes more diffused and peaks at a lower value. Apart from that, the evolution is very similar to the earlier case.

The total energy associated with the field configuration can be obtained by integrating u over all space. The total energy turns out to be $Energy = 2\pi^2/a\mu_0$.

Of course we can redefine F to get a different energy scale. $F = \nabla(a\alpha) \times \nabla(b\beta)$, where a and b are real constants. The electric and magnetic field gets scaled by ab and energy density by $(ab)^2$.

The Poynting vector can be obtained using, $\mathbf{S} = \frac{1}{\mu_0} \mathbf{E} \times \mathbf{B}$.

$$\mathbf{S} = \frac{16 a^4 c}{\mu_0} \left(\frac{2(ay - xz)}{(x^2 + y^2 + z^2 + a^2)^5}, -\frac{2(ax + yz)}{(x^2 + y^2 + z^2 + a^2)^5}, \frac{x^2 + y^2 - z^2 - a^2}{(x^2 + y^2 + z^2 + a^2)^5} \right) \quad (3.6)$$

Comparing with the form of electric field and magnetic field, it is clear that Poynting vector too has a knotted structure. Now we can compute the total momentum of the system using $\mathbf{P} = \epsilon_0 \mu_0 \int \mathbf{S} d\tau$. The x and y component would give zero when integrating over all space, as both are odd functions in one or more of variables x , y and z . The z component integrates to $-\pi^2 c \epsilon_0 / a$.

$$\mathbf{P} = \left(0, 0, \frac{-\pi^2 c \epsilon_0}{a} \right) \hat{z} \quad (3.7)$$

If we assume that the field structure is a particle, then the rest mass of the particle turns out to be around $\frac{\sqrt{3}\pi^2 \epsilon_0}{a}$. We can also compute the angular momentum associated with the system is.

Angular momentum density is given by $\mathbf{l} = \epsilon_0 \int \mathbf{r} \times \mathbf{S} d\tau$.

$$\mathbf{l} = 16c\epsilon_0 a^4 \left(\frac{y(x^2 + z^2 - a^2) + 2axz + y^3}{(x^2 + y^2 + z^2 + a^2)^5}, \frac{-(x^3 + x(y^2 + z^2 - a^2) - 2ayz)}{(x^2 + y^2 + z^2 + a^2)^5}, \frac{-2a(x^2 + y^2)}{(x^2 + y^2 + z^2 + a^2)^5} \right) \quad (3.8)$$

Again, x and y component would give zero upon integration over all space. The z component gives $-\pi^2 c\epsilon_0$.

$$\mathbf{L} = -\pi^2 c\epsilon_0 \hat{z} \quad (3.9)$$

Chapter 4

Properties

In this chapter we study some of the classical properties of the solution obtained above, especially for the case $p = 1$ and $q = 1$.

4.1 Reflection

We study the reflection of hopfion from a conducting plane at normal incidence. The electric field inside a perfect conductor is zero. This results in the following boundary conditions at the surface of a conductor.

$$\hat{n} \times \mathbf{E} = 0 \quad (4.1a)$$

$$\hat{n} \times \mathbf{H} = \mathbf{K} \quad (4.1b)$$

$$\hat{n} \cdot \mathbf{D} = \sigma \quad (4.1c)$$

$$\hat{n} \cdot \mathbf{B} = 0 \quad (4.1d)$$

Where $H = B/\mu_0$ and $D = \epsilon_0 E$. σ and \mathbf{K} are induced surface charge density and surface current density respectively. At the surface of conductor, the tangential component of electric field and normal component of magnetic field are zero. The normal component of electric field is proportional to the surface charge density and tangential component of magnetic field is proportional to the current induced at the surface of conductor. This suggests the following transformations to obtain the reflected field, for the case when conducting plane is at $z = 0$.

$$E_R(x, y, z, t) = (-E_x(x, y, -z, t), -E_y(x, y, -z, t), E_z(x, y, -z, t)) \quad (4.2a)$$

$$B_R(x, y, z, t) = (B_x(x, y, -z, t), B_y(x, y, -z, t), -B_z(x, y, -z, t)) \quad (4.2b)$$

The transformation suggests that the tangential component of electric field of the reflected wave switches direction with respect to the incident wave. The normal component of electric field remains the same. On the other hand, for magnetic fields the tangential component remains the same and

normal components switches direction. Let us check whether this transformation works for plane waves. Consider the following figure. The direction of propagation is shown in blue, magnetic field in orange and electric field in red. The direction can be obtained by imposing orthogonality of electric field, magnetic field and Poynting vector, $E \times B \sim K$.

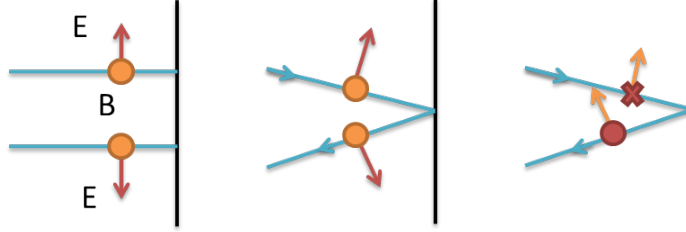


Figure 4.1: Reflection of plane wave

- Case 1: Normal Incidence.

At the surface of the conductor electric field and magnetic field both have only tangential components. The electric field of reflected wave switches direction with respect to the incident wave, while the direction of magnetic field remains the same. This is in accord with transformation in equation 4.2.

- Case 2: Oblique Incidence. Electric field lies in the plane of paper.

Magnetic field is tangential and it doesn't change direction. Electric field has both normal and tangential components. The tangential component switches direction while normal component doesn't.

- Case 3: Oblique Incidence. Magnetic field lies in the plane of paper.

Electric field has only tangential component, which switches direction. The normal component of magnetic field switches direction while tangential component remain the same.

Linearly polarized plane waves seem to follow the transformation 4.2 when reflected from a conducting plane at $z = 0$.

The charge and current induced on the surface of conductor due to the boundary conditions gives rise to the reflected wave. We show this explicitly for the case of normal incidence. Consider the following incident wave.

$$\mathbf{E} = E_0 \cos(\omega t - kz)\hat{x} \quad (4.3a)$$

$$\mathbf{B} = \frac{E_0}{c} \cos(\omega t - kz)\hat{y} \quad (4.3b)$$

The reflecting surface is at $z = 0$. Using 4.2 we obtain the following form of reflected wave.

$$\mathbf{E}_r = -E_0 \cos(\omega t + kz)\hat{x} \quad (4.4a)$$

$$\mathbf{B}_r = \frac{E_0}{c} \cos(\omega t + kz)\hat{y} \quad (4.4b)$$

Now we can use the boundary conditions in equation 4.1 to obtain the following form for induced surface charge and current.

$$\sigma = 0 \quad (4.5a)$$

$$\mathbf{K} = 2 \frac{E_0}{c \mu_0} \cos(\omega t) \hat{x} \quad (4.5b)$$

We can obtain the retarded potential using the following formulae.

$$V(\vec{r}, t) = \frac{1}{4\pi\epsilon_0} \int d^3x' \frac{\rho(\vec{r}', t_r)}{|\vec{r} - \vec{r}'|} \quad (4.6a)$$

$$\mathbf{A}(\vec{r}, t) = \frac{\mu_0}{4\pi} \int d^3x' \frac{\mathbf{J}(\vec{r}', t_r)}{|\vec{r} - \vec{r}'|} \quad (4.6b)$$

Where, $t_r = t - |\vec{r} - \vec{r}'|/c$ is the retarded time. Clearly, the scalar potential will be zero as there is no induced charge density. To compute the vector potential at $(0, 0, z)$ for $z < 0$, consider the following figure (fig. 4.2).

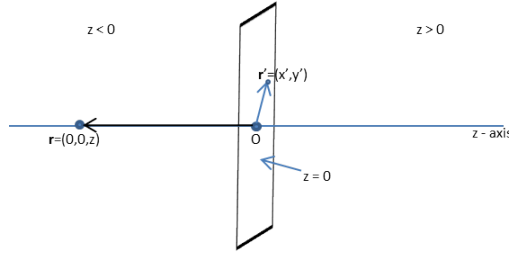


Figure 4.2: Computing retarded potentials

$$\begin{aligned} \mathbf{A}(\vec{r}, t) &= \frac{2E_0\mu_0}{4\pi c\mu_0} \int \int \rho' d\rho' d\theta' \frac{\cos\left(\omega\left(t - |\vec{r} - \vec{r}'|/c\right)\right)}{|\vec{r} - \vec{r}'|} \hat{x} \\ &= \frac{E_0}{c} \int_0^\infty \rho' d\rho' \frac{\cos\left(\omega\left(t - (\rho'^2 + z^2)^{1/2}/c\right)\right)}{(\rho'^2 + z^2)^{1/2}} \hat{x} \end{aligned}$$

Define, $u^2 = \rho'^2 + z^2$. Then $udu = \rho' d\rho'$. For negative z , the limits of integration changes from $0 \rightarrow \infty$ to $-z \rightarrow \infty$. Making the mentioned substitution in the integral results in the following.

$$\begin{aligned} \mathbf{A}(\vec{r}, t) &= \frac{E_0}{c} \int_{-z}^\infty u du \frac{\cos(\omega(t - u/c))}{u} \hat{x} \\ &= \frac{E_0}{c} \int_{-z}^\infty du \cos(\omega(t - u/c)) \hat{x} \\ &= \frac{E_0}{\omega} \sin(\omega t + kz) \hat{x} + const \end{aligned}$$

Now we can determine the electric field and magnetic field from the scalar and vector potentials using following formulae.

$$\mathbf{E} = -\nabla V - \frac{\partial \mathbf{A}}{\partial t} \quad (4.9a)$$

$$\mathbf{B} = \nabla \times \mathbf{A} \quad (4.9b)$$

We get back the reflected wave.

$$\mathbf{E} = -E_0 \cos(\omega t + kz) \hat{x} \quad (4.10a)$$

$$\mathbf{B} = \frac{E_0}{c} \cos(\omega t + kz) \hat{y} \quad (4.10b)$$

This proves that the transformation 4.2 works very well for plane waves, at least for normal incidence. Applying the same transformation to the hopfion ($p = 1, q = 1$) solution, we get the following form for the electric and magnetic fields at $t = 0$.

$$\mathbf{E}_R = c \left(\frac{4(x^2 - y^2 - z^2 + 1)}{(x^2 + y^2 + z^2 + 1)^3}, \frac{8(xy + z)}{(x^2 + y^2 + z^2 + 1)^3}, -\frac{8(y - xz)}{(x^2 + y^2 + z^2 + 1)^3} \right) \quad (4.11a)$$

$$\mathbf{B}_R = \left(\frac{8xy - 8z}{(x^2 + y^2 + z^2 + 1)^3}, -\frac{4(x^2 - y^2 + z^2 - 1)}{(x^2 + y^2 + z^2 + 1)^3}, \frac{8(x + yz)}{(x^2 + y^2 + z^2 + 1)^3} \right) \quad (4.11b)$$

To check whether the reflected field also have knotted structure, we need to find an analogue of ψ_E and ψ_B introduced in chapter 3.

$$\nabla \psi_E(x, y, z, t) \cdot \mathbf{E}(x, y, z, t) = 0 \quad (4.12a)$$

$$\nabla \psi_B(x, y, z, t) \cdot \mathbf{B}(x, y, z, t) = 0 \quad (4.12b)$$

We need to find ψ_E^r and ψ_B^r , such that,

$$\nabla \psi_E^r(x, y, z, t) \cdot \mathbf{E}_R(x, y, z, t) = 0 \quad (4.13a)$$

$$\nabla \psi_B^r(x, y, z, t) \cdot \mathbf{B}_R(x, y, z, t) = 0 \quad (4.13b)$$

Using transformation 4.2, we can re-write equation 4.13(a) as follows.

$$\begin{aligned} & \nabla \psi_E^r \cdot (-E_x(x, y, -z, t), -E_y(x, y, -z, t), E_z(x, y, -z, t)) = 0 \\ \Rightarrow & -\frac{\partial \psi_E^r(x, y, z, t)}{\partial x} E_x(x, y, -z, t) - \frac{\partial \psi_E^r(x, y, z, t)}{\partial y} E_y(x, y, -z, t) + \frac{\partial \psi_E^r(x, y, z, t)}{\partial z} E_z(x, y, -z, t) = 0 \end{aligned}$$

Now if we make the transformation $z \rightarrow -z$ we get,

$$-\frac{\partial \psi_E^r(x, y, -z, t)}{\partial x} E_x(x, y, z, t) - \frac{\partial \psi_E^r(x, y, -z, t)}{\partial y} E_y(x, y, z, t) - \frac{\partial \psi_E^r(x, y, -z, t)}{\partial z} E_z(x, y, z, t) = 0$$

This is same as,

$$\nabla\psi_E^r(x, y, -z, t) \cdot \mathbf{E} = 0$$

Comparing with equation 4.12(a) it is clear that $\psi_E^r(x, y, z, t) = \psi_E(x, y, -z, t)$. A similar analysis for equation 4.13(b) can be done to obtain ψ_B^r . This time we will have,

$$\nabla\psi_E^r \cdot (B_x(x, y, -z, t), B_y(x, y, -z, t), -B_z(x, y, -z, t)) = 0$$

After $z \rightarrow -z$ transformation we will get,

$$\frac{\partial\psi_B^r(x, y, -z, t)}{\partial x} B_x(x, y, z, t) - \frac{\partial\psi_B^r(x, y, -z, t)}{\partial y} B_y(x, y, z, t) - \frac{\partial\psi_B^r(x, y, -z, t)}{\partial z} B_z(x, y, z, t) = 0$$

Again we get a similar form.

$$\nabla\psi_B^r(x, y, -z, t) \cdot \mathbf{B} = 0$$

Comparing with equation 4.12(b) it is clear that $\psi_B^r(x, y, z, t) = \psi_B(x, y, -z, t)$. Re-writing the results.

$$\psi_E^r(x, y, z, t) = \psi_E(x, y, -z, t) \tag{4.14a}$$

$$\psi_B^r(x, y, z, t) = \psi_B(x, y, -z, t) \tag{4.14b}$$

We plot the surfaces of constant ψ_B^r for $p = 1$ and $q = 1$.

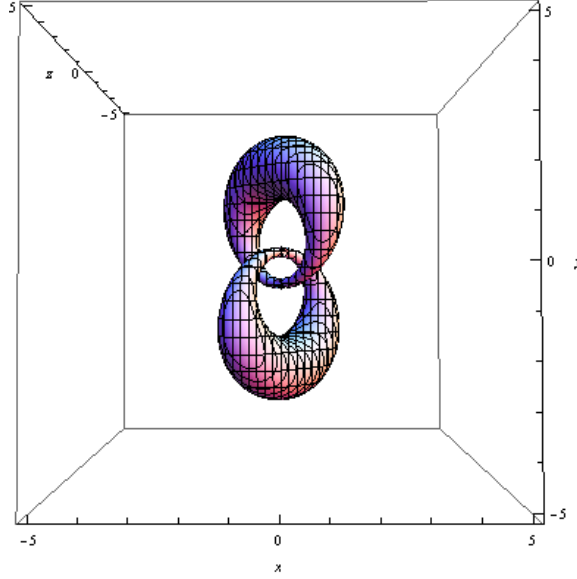


Figure 4.3: $\psi_B^r = 0.45$ and $\psi_B^r = -0.45$ for $p = 1$ and $q = 1$.

We can see that the reflected fields also have knotted structure.

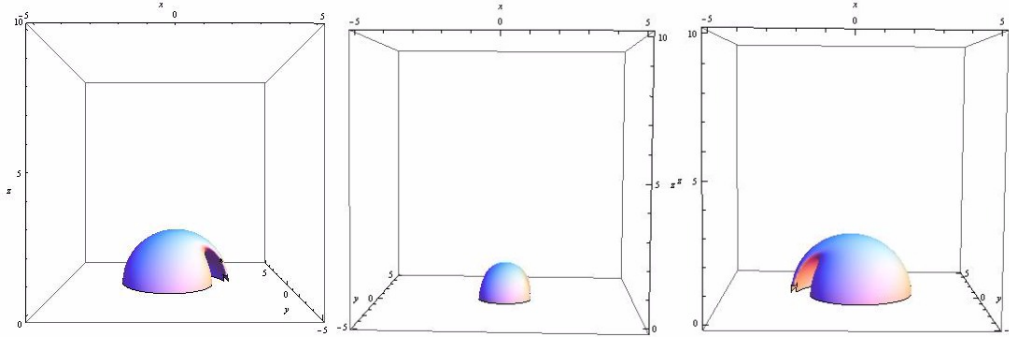


Figure 4.4: Evolution of energy iso-surfaces of total electromagnetic field. $t = -2$, $t = 0$ and $t = 2$ respectively.

As in the case of plane waves, we can compute the charge and current density induced on the conducting plane surface. At $t = 0$ we get the following results.

$$\sigma = -\frac{16y}{(x^2 + y^2 + 1)^3} \quad (4.15a)$$

$$\mathbf{K} = \frac{16xy}{(x^2 + y^2 + 1)^3} \hat{x} + \frac{8(-x^2 + y^2 + 1)}{(x^2 + y^2 + 1)^3} \hat{y} \quad (4.15b)$$

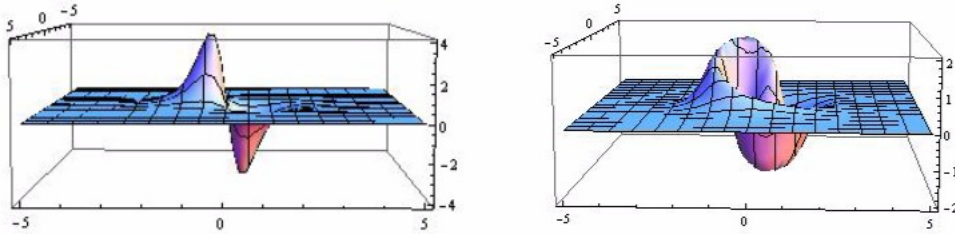


Figure 4.5: Evolution of surface charge density. $t = 0$ and $t = 1$ respectively.

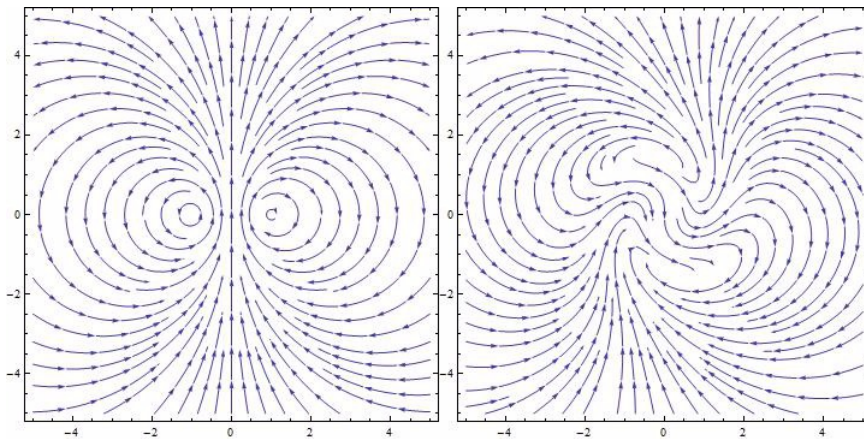


Figure 4.6: Evolution of surface current density. $t = 0$ and $t = 1$ respectively.

The induced charge and current densities must produce the reflected field. We can use equations 4.6 and 4.9 to check whether we get back the reflected wave. But due to the complicated form of surface charge and current densities, we were unable to compute the integrals.

4.2 Particle Trajectory

We plot the trajectory of a particle in presence of knotted electromagnetic field corresponding to $p = 1$ and $q = 1$. The initial conditions are, $x = 1, y = 1, z = 0, \mathbf{v} = 0$ at $t = 0$.

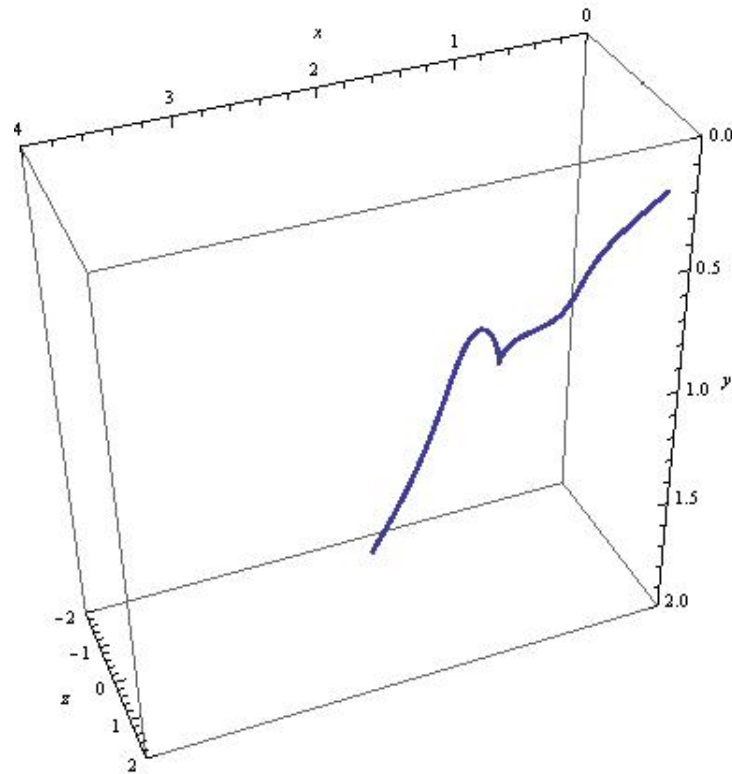


Figure 4.7: Trajectory of a particle in presence of knotted field.

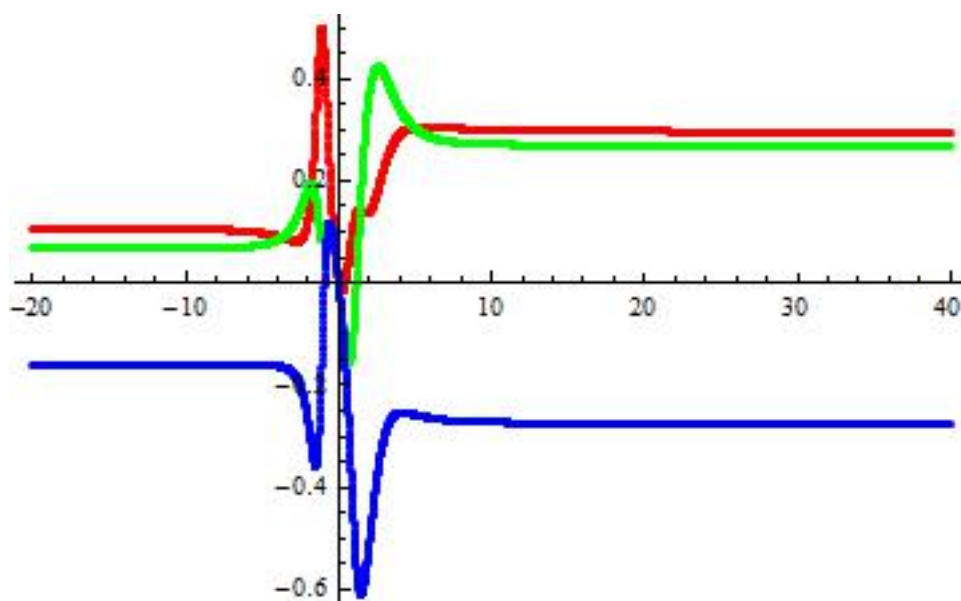


Figure 4.8: Velocity vs time. Red is x component of velocity, green is y and blue is z

4.3 Emf induced

In this section we study the emf induced in a coil in presence of knotted electromagnetic field. We choose a square coil placed on the plane $x = 0$. The vertices are at $(0,1,1)$, $(0,1,-1)$, $(0,-1,1)$ and $(0,-1,-1)$. The emf induced on a coil is given by,

$$\text{emf} = \oint \mathbf{E} \cdot d\mathbf{l} \quad (4.16)$$

Using Stoke's theorem we can write,

$$\text{emf} = \int_{\Omega} \nabla \times \mathbf{E} \cdot d\mathbf{A} = - \int_{\Omega} \frac{\partial \mathbf{B}}{\partial t} \cdot d\mathbf{A} \quad (4.17)$$

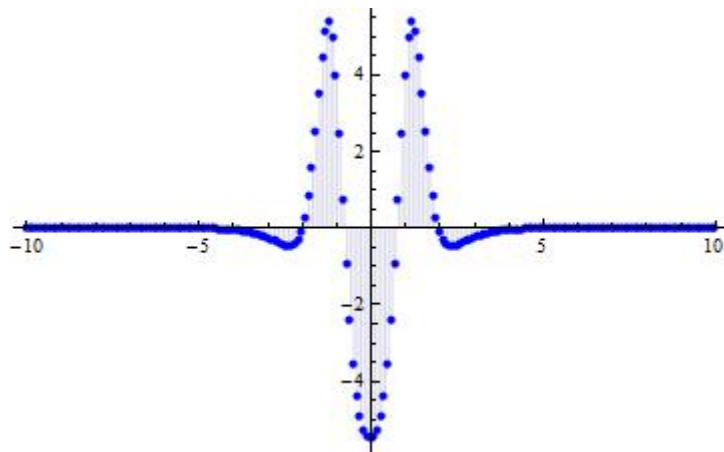


Figure 4.9: Induced emf due to the presence of knotted field.

Chapter 5

Formalism

5.1 Covariant Formalism

In this section we express the Bateman's construction covariantly[7]. Using index notation we can re-write equation 1.4 as,

$$E^i + iB^i = \epsilon^{ijk} \partial_j \alpha \partial_k \beta \quad (5.1)$$

If $F^{\mu\nu}$ is the electromagnetic field tensor, equation 5.1 can be written as,

$$F^{0i} + \frac{i}{2} \epsilon^{ijk} F_{jk} = \epsilon^{ijk} \partial_j \alpha \partial_k \beta$$

Where E^i is F^{0i} and B^i is $\frac{i}{2} \epsilon^{ijk} F_{jk}$. Defining $\epsilon_{0ijk} = \epsilon_{ijk}$ and $\epsilon^{0ijk} = -\epsilon^{ijk}$, we get the following as the covariant form.

$$F^{\mu\nu} - \frac{i}{2} \epsilon^{\mu\nu\alpha\beta} F_{\alpha\beta} = -\epsilon^{\mu\nu\rho\sigma} \partial_\rho \alpha \partial_\sigma \beta \quad (5.2)$$

The i,j component of the equation 5.2 gives.

$$\begin{aligned} F^{ij} - i\epsilon^{ijk0} F_{k0} &= -\epsilon^{ijk0} (\partial_k \alpha \partial_0 \beta - \partial_0 \alpha \partial_k \beta) \\ \epsilon^{ijk} B_k - i\epsilon^{ijk} E_k &= \epsilon^{ijk} (\partial_t \alpha \partial_k \beta - \partial_k \alpha \partial_t \beta) \\ B_k - iE_k &= (\partial_t \alpha \partial_k \beta - \partial_k \alpha \partial_t \beta) \\ E_k + iB_k &= (\partial_t \alpha \partial_k \beta - \partial_k \alpha \partial_t \beta) \end{aligned}$$

Comparing this with equation 5.1, we can see that Bateman's condition is already encoded in equation 5.2. Hence it contains all the information about equations of motions. We can also write down the four vector potential in terms of α and β .

$$\epsilon^{\mu\nu\alpha\beta} F_{\alpha\beta} = -2\epsilon^{\mu\nu\rho\sigma} \text{Im}[\partial_\rho \alpha \partial_\sigma \beta]$$

We can use the identity,

$$\epsilon_{\mu\nu\rho_1\sigma_1}\epsilon^{\mu\nu\rho_2\sigma_2} = -2(\delta_{\rho_1}^{\rho_2}\delta_{\sigma_1}^{\sigma_2} - \delta_{\sigma_1}^{\rho_2}\delta_{\rho_1}^{\sigma_2}) \quad (5.3)$$

to get the following results.

$$F_{\mu\nu} = \text{Im}[\partial_\mu\alpha\partial_\nu\beta - \partial_\nu\alpha\partial_\mu\beta] \quad (5.4)$$

$$= \partial_\mu A_\nu - \partial_\nu A_\mu \quad (5.5)$$

$$A_\mu = \text{Im}[H_\mu] \quad (5.6)$$

$$H_\mu = \frac{1}{2}(\alpha\partial_\mu\beta - \beta\partial_\mu\alpha) \quad (5.7)$$

5.2 Map to SU(2) gauge theories

Quaternions

Quaternions are extension of complex numbers. It has 4 basis elements: 1, i, j and k. The product rules are: $i^2 = j^2 = k^2 = ijk = -1$, $ij = k$ and cyclic terms, $ji = -k$ and cyclic terms. We can find a representation for the basis using 2 dimensional Pauli matrices: $1 = \mathbf{I}_{2\times 2}$, $i = -i\sigma_1$, $j = -i\sigma_2$ and $k = -i\sigma_3$. Defining,

$$\mathbf{q} = \frac{1}{m}(\alpha + \beta j) = \frac{1}{m}(\alpha_0 + i\alpha_1 + (\beta_0 + i\beta_1)j) = \frac{1}{m}(\alpha_0 + i\alpha_1 + j\beta_0 + k\beta_1) \quad (5.8)$$

$$\mathbf{q}^* = \frac{1}{m}(\alpha_0 - i\alpha_1 - j\beta_0 - k\beta_1) = \frac{1}{m}(\alpha_0 - i\alpha_1 - j(\beta_0 + i\beta_1)) = \frac{1}{m}(\alpha^* - \beta j) \quad (5.9)$$

where $m = \sqrt{|\alpha|^2 + |\beta|^2} = 1$. Also, $\mathbf{q}\mathbf{q}^* = 1$. Defining quaternionic potential as follows.[7]

$$\mathbf{Q}_\mu = \mathbf{q}\partial_\mu\mathbf{q}^* \quad (5.10)$$

$$\mathbf{Q}_\mu^* = \mathbf{q}^*\partial_\mu\mathbf{q} = \partial_\mu(\mathbf{q}\mathbf{q}^*) - \mathbf{q}\partial_\mu\mathbf{q}^* = -\mathbf{Q}_\mu \quad (5.11)$$

As, $\partial_\mu(\mathbf{q}\mathbf{q}^*) = 0$. The quaternionic potential can be simplified to following.

$$\begin{aligned} [\mathbf{Q}_\mu, \mathbf{Q}_\nu] &= (\mathbf{q}\partial_\mu\mathbf{q}^*)(\mathbf{q}\partial_\nu\mathbf{q}^*) - (\mathbf{q}\partial_\nu\mathbf{q}^*)(\mathbf{q}\partial_\mu\mathbf{q}^*) \\ &= (\partial_\mu(\mathbf{q}\mathbf{q}^*) - (\partial_\mu\mathbf{q})\mathbf{q}^*)\mathbf{q}\partial_\nu\mathbf{q}^* - (\partial_\nu(\mathbf{q}\mathbf{q}^*) - (\partial_\nu\mathbf{q})\mathbf{q}^*)\mathbf{q}\partial_\mu\mathbf{q}^* \end{aligned}$$

We get,

$$[\mathbf{Q}_\mu, \mathbf{Q}_\nu] = -(\partial_\mu\mathbf{q}\partial_\nu\mathbf{q}^* - \partial_\nu\mathbf{q}\partial_\mu\mathbf{q}^*) \quad (5.12)$$

$$\partial_\mu\mathbf{Q}_\nu - \partial_\nu\mathbf{Q}_\mu = \partial_\mu(\mathbf{q}\partial_\nu\mathbf{q}^*) - \partial_\nu(\mathbf{q}\partial_\mu\mathbf{q}^*) = (\partial_\mu\mathbf{q}\partial_\nu\mathbf{q}^* - \partial_\nu\mathbf{q}\partial_\mu\mathbf{q}^*) \quad (5.13)$$

The field strength is given by $\mathbf{Q}_{\mu\nu} = \partial_\mu\mathbf{Q}_\nu - \partial_\nu\mathbf{Q}_\mu + [\mathbf{Q}_\mu, \mathbf{Q}_\nu] = 0$. Hence it is a pure gauge solution.

5.3 Gauge Transformation

In this section we explore the gauge freedom with respect to Bateman's variables, α and β . We consider infinitesimal gauge transformation of the 4-vector potential.

$$A_\mu \rightarrow A'_\mu = A_\mu + \partial_\mu(c\theta) \quad (5.14)$$

Where c and θ are real functions. The general infinitesimal transformation for α and β is.

$$\alpha \rightarrow \alpha' = \alpha + 4ia\alpha\theta \quad (5.15a)$$

$$\beta \rightarrow \beta' = \beta + 4ib\beta\theta \quad (5.15b)$$

A factor of $4i$ has been kept for later convenience. Using equation 5.6 we get.

$$\begin{aligned} A_\mu &= \frac{H_\mu - H_\mu^*}{2i} = \frac{1}{4i} ((\alpha\partial_\mu\beta - \beta\partial_\mu\alpha) - c.c.) \\ \delta A_\mu &= \frac{1}{4i} ((\delta\alpha\partial_\mu\beta + \alpha\partial_\mu(\delta\beta) - \delta\beta\partial_\mu\alpha - \beta\partial_\mu(\delta\alpha)) - c.c.) \\ c\partial_\mu\theta + (\partial_\mu c)\theta &= \frac{1}{4i} ((4ia\alpha\theta\partial_\mu\beta + \alpha\partial_\mu(4ib\beta\theta) - 4ib\beta\theta\partial_\mu\alpha - \beta\partial_\mu(4ia\alpha\theta)) - c.c.) \\ c\partial_\mu\theta + (\partial_\mu c)\theta &= ((a\alpha\theta\partial_\mu\beta + \alpha\partial_\mu(b\beta\theta) - b\beta\theta\partial_\mu\alpha - \beta\partial_\mu(a\alpha\theta)) + c.c.) \end{aligned}$$

Where *c.c.* denotes complex conjugate. In the last step the sign of complex conjugate term has been changed as we have taken i outside the bracket. Equating the coefficient of θ and $\partial_\mu\theta$ on both sides of last equation gives the following result.

$$c = \alpha\beta(b - a) + c.c. \quad (5.16a)$$

$$\partial_\mu c = (\alpha\beta\partial_\mu b - \alpha\beta\partial_\mu a + \alpha b\partial_\mu\beta - \alpha a\partial_\mu\beta + \beta b\partial_\mu\alpha - \beta a\partial_\mu\alpha) + c.c. \quad (5.16b)$$

Taking the derivative of equation 5.13(a) and subtracting with equation 5.13(b) would give the following consistency condition.

$$(a\alpha\partial_\mu\beta - b\beta\partial_\mu\alpha) + c.c. = 0 \quad (5.17)$$

This is a very restricting condition. For instance if we ignore the complex conjugate term, then the above condition implies $\partial_\mu\beta = f(\vec{x}, t)\partial_\mu\alpha$. This implies $\partial_\mu\alpha\partial_\nu\beta$ is symmetric. Hence right hand side of equation 5.2 becomes zero (As we are contracting symmetric tensor with an anti-symmetric tensor). So, field strength is zero. Alternatively, it would imply $\nabla\alpha$ is proportional to $\nabla\beta$. Hence their cross product would be zero. This implies that F in equation 1.8 is zero. Again we get the same conclusion that the field strength is zero. So, prime-facie it appears that Bateman's variables doesn't exhibit gauge freedom for a general field configuration. But the involvement of complex conjugate terms demands analysis in greater detail, which we haven't been able to complete due to time constraints.

Bibliography

- [1] H. Bateman, *Mathematical Analysis of Electrical and Optical Wave-Motion*. New York: Dover, 1915.
- [2] W. T. M. Irvine, H. Kedia, I. Bialynicki-Birula, and D. Peralta-Salas, “Tying Knots in Light Fields,” *PRL*, vol. 111, 2013.
- [3] W. B. R. Lickorish, *An Introduction to Knot Theory*. New York: Springer, 1991.
- [4] C. C. Adams, *The Knot Book*. Hyderabad: Univerities Press (India) Pvt. Ltd., 2012.
- [5] J. Milnor, *Singular Points on Complex Hypersurfaces*. New Jersey: Princeton University Press, 1969.
- [6] W. T. M. Irvine and D. Bouwmeester, “Linked and Knotted Beams of Light,” *Nature Physics*, vol. 4, pp. 716–720, 2008.
- [7] J. Sonnenschein, C. Hoyos, and N. Sircar, “New Knotted Solutions of Maxwell’s Equations,” *ArXiv*, vol. 1502.01382v1, 2015.